Micrometer-Scale Translation and Monitoring of Individual Nanocars on Glass

Saumyakanti Khatua, Jason M. Guerrero, Kevin Claytor, Guillaume Vives, Anatoly B. Kolomeisky, James M. Tour,* and Stephan Link*

Department of Chemistry and the Smalley Institute for Nanoscale Science and Technology, Rice University, 6100 Main Street, Houston, Texas 77005

ABSTRACT Nanomachines designed to exhibit controlled mechanical motions on the molecular scale present new possibilities of building novel functional materials. Single molecule fluorescence imaging of dye-labeled nanocars on a glass surface at room temperature showed a coupled translational and rotational motion of these nanoscale machines with an activation energy of 42 ± 5 kJ/mol. The 3 nm-long dye-labeled carborane-wheeled nanocars moved by as much as 2.5 μm with an average speed of 4.1 nm/s. Translation of the nanocars due a wheel-like rolling mechanism is proposed and this is consistent with the absence of movement for a three-wheeled nanocar analogue and the stationary behavior of unbound dye molecules. These findings are an important first step toward the rational design and ultimate control of surface-operational molecular machines.

Science and engineering on the nanoscale offers novel possibilities for the design and synthesis of functional materials. In contrast to the engineering of macroscopic objects where large pieces of materials are formed into smaller building blocks, nanoscale engineering is driven by a bottom-up materials synthesis. Inspiration for this approach can be drawn from nature where self-assembly of smaller molecules into larger networks through often weak interactions play an important role. Nanomachines are promising new devices that are designed to exhibit controlled mechanical motions resembling macroscopic rotors,[1−4] elevators,[5] shuttles,[6−8] ratchets,[9] turnstiles,[10] scissors,[11] and muscles.[12] Performing electronic and mechanical operations with specifically designed molecules presents the ultimate limit of miniaturization and has a profound impact on many diverse fields ranging from molecular computing to medicine. Among the most important tasks for molecular machines is the directed transport of molecules and charges. To accomplish molecular directed motion and transport, molecular machines that resemble the chassis and wheels of a car, hence called nanocars, have been synthesized.[13−15] The rotation of the nanocar wheels is thought to induce a directional rolling of the nanocars on a surface.[15] Understanding the mechanisms by which these molecular machines work under different conditions is crucial for the future design of even more complex machines and essential for finding novel ways to control the forces that are responsible for their mechanical nanoscale motion.

Ensemble characterization techniques often fail to measure the detailed mechanical action of molecular machines as a random alignment of the individual molecules can lead to an orientational averaging, which is particularly problematic for the two-dimensional motion of a nanocar on a flat surface. Thermally activated rolling of individual fullerene-wheeled nanocars has previously been studied by scanning tunneling spectroscopy (STM) on a gold surface.[15] While STM is extremely powerful in resolving atomic scale details of single molecules,[16] the substrate surface must be conductive. As a complementary single molecule technique, fluorescence imaging[17−19] is capable of monitoring the motion of single molecules on nonconductive glass. Although the resolution of optical single molecule spectroscopy is limited by diffraction, localization of individual molecules below 100 nm down to a few nanometers has become possible for large photon count rates[17,19] while, at the same time, acquiring images that are tens of micrometers large.

Here, we report on the translational motion of single dye-labeled carborane-wheeled nanocars on a glass surface, studied for the first time by single molecule fluorescence spectroscopy. Using polarization sensitive fluorescence detection in
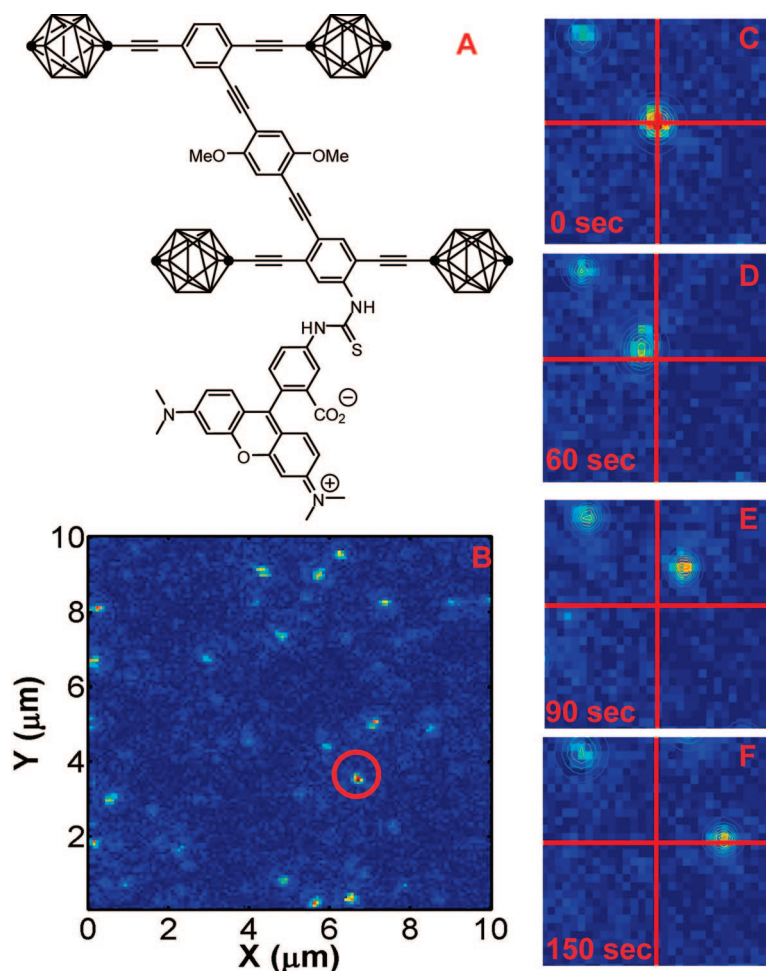
Figure 1. (A) Dye-labeled four-wheeled nanocar. The vertices in the carborane wheels correspond to B−H units while the black dots correspond to C and C−H units, ipso and para, respectively. The nanocar is ~2 × 2 nm and the dye "trailer" is ~1 × 1 nm. (B) Fluorescence image (10 μm × 10 μm, 128 × 128 pixels, 1 ms/pixel, $\lambda_{exc.}$ = 532 nm, 1 kW/cm^2) of single nanocars. (C−F) Time-lapse images (2.3 μm × 2.3 μm) for the nanocar circled in (B) demonstrating movement of the nanocar at room temperature. The red cross hair provides a stationary reference point.

nanocars were isolated on a glass surface by spin-casting from a 10^{-12} mol/L dimethylformamide (DMF) solution. Single photobleaching steps in fluorescence-time trajectories confirmed the presence of single molecules within the diffraction limited fluorescence signal.[19] The 10 μm × 10 μm fluorescence images were acquired by scanning the sample over a focused laser beam in a home-built confocal microscope setup (Figure 1B). Movement of a single nanocar is shown in the images in Figure 1C−F. The images were acquired continuously every 30 s for a total time of 5 min.

Single nanocar trajectories were obtained by an automated routine that first identified individual molecules on the basis of the intensity and size (e.g., number of pixels) of the fluorescent spot in the starting image for a time series of frames. If a molecule is found at the same position or within a search area in the subsequent frame, the molecule is associated with the corresponding one in the previous image. This procedure is repeated for all molecules and every frame. Large displacements within the relatively long image acquisition time of 30 s, photoblinking of the dye, and high single molecule coverage could lead to an incorrect association. Photoblinking was addressed by searching in subsequent frames for molecules that blink on again. However, if an unambiguous assignment could not be made the corresponding molecules were excluded from further analysis. In addition, the dimensions of the search area and the concentration of nanocars were carefully adjusted to minimize intersecting search regions. A typical search radius was 600 nm for images with coverages of 10−15 molecules per 100 μm^2. Figure 2A shows the first analyzed frame of a time series of fluorescence images for carborane-wheeled nanocars together with superimposed trajectories obtained from the following images demonstrating that the displacements of individual nanocars can be as large as 500 nm between frames.

A nonspecific movement of individual molecules on glass can be excluded here because fluorescence imaging of the dye only showed no measurable displacements outside our experimental error. We repeated the same single molecule experiments and analysis for individual TRITC molecules isolated on a glass surface (Figure 2B). The TRITC by itself showed no translational motion, which can be seen from the comparison of two typical trajectories obtained for the nanocar and TRITC (Figure 2C). The magnified nanocar trajectory in Figure 2C includes the error bars calculated from fitting each fluorescence spot to the microscope point spread function, which was approximated as a two-dimensional

combination with a comparative analysis that employed three-wheeled nanocars and the dye tag only, we were able to investigate possible mechanisms for the movement of carborane-wheeled nanocars. Our results are consistent with a wheel-like rolling of the nanocars.

RESULTS AND DISCUSSION

Fluorescence visualization of the nanocars with 532 nm excitation light was achieved by first attaching an appropriate dye label (tetramethylrhodamine isothiocyanate, TRITC) to the end of the nanocar chassis (Figure 1A). TRITC tagging of the nanocars was accomplished through an aniline-bearing nanocar reacting with the isothiocyanate residue on the fluorophore (Supporting Information). At room temperature without thermal activation, the dye-labeled carborane-wheeled nanocars showed significant displacement in successively scanned fluorescence images directly confirming movement of the nanocars on a glass surface. Individual

Gaussian.[18,19] For TRITC, the displacements are comparable or even smaller than the error bars verifying that the TRITC molecules remained stationary. On the other hand, the movement of the nanocars is much larger than our spatial resolution of 100 nm. The resolution is mainly limited by photon shotnoise and photoblinking of the dye as well as a pixel size of 78 nm.[18] Despite a longer image acquisition time and reduced spatial resolution, the main advantage of our confocal sample scanning setup over wide-field imaging is that a nonconstant laser illumination of all molecules allowed us to extend the total acquisition time and to obtain trajectories spanning several minutes.

It is interesting to note from Figure 2A that not all molecules that were identified actually moved. In fact, about 25% of the nanocars (46 out of 191 molecules) showed translational motion, which further illustrates the power and need for single molecule measurement techniques. A main factor contributing to the large fraction of nonmoving nanocars is most likely the surface roughness of the glass surface as it is not atomically flat; it is merely a glass coverslip (Fisher Scientific, 12-545-F) and the nanocars could become lodged at lattice defects. AFM measurements of a glass coverslip confirmed both smooth areas and surface height modulations of several nanometers exceeding the dimensions of the nanocars. Second, a fluorescent spot only indicates the presence of TRITC, which by itself did not move (Figure 2B), and the presence of some nonlinked TRITC molecules due to decomposition cannot be excluded. In the following, we will concentrate only on the nanocars that showed a displacement which exceeded the error bar in at least 2 image frames. These moving nanocars are colored red in Figure 2A. However, the nonmoving nanocars colored yellow in Figure 2A served the important role of an internal marker against overall sample drift. We found that sample drift (inset in Figure 2D) was 11 nm during the experiment shown in Figures 1 and 2, which is much smaller than the micrometer-scale movement of the nanocars as well as our spatial resolution of 100 nm.

We observed no biased movement of the nanocars on this amorphous surface. A histogram of angles obtained from the single molecule trajectories for all moving nanocars showed an equal distribution of all angles between 0 and 180 degrees (Figure S1). Polarization anisotropy analysis of the fluorescence images furthermore revealed that the nanocars, when they changed directions, underwent the change rapidly and within the time it took to scan the molecule over the laser beam (~500 ms, Figure 3A). The polarization anisotropy distribution of the nanocars is peaked at zero indicating depolarization due to rotational movement. A rotation of the TRITC on the nanocar can be excluded as the major depolarization mechanism because an analysis of only the center pixel showed a broader polarization distribution (Figure S2). This is consistent with rota-
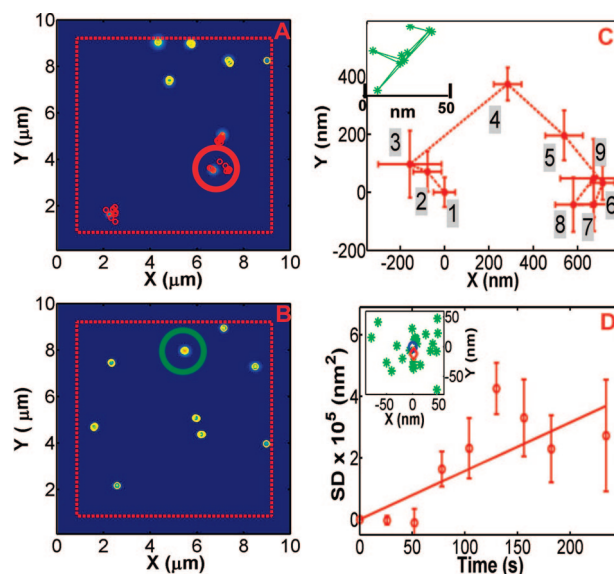

Figure 2. Analyzed images of nanocar (A) and TRITC (B). Molecules were identified on the basis of intensity and size within the region marked by the red box. The positions of the molecules for a time series of images are shown superimposed on the first frame; 25% of the nanocars showed displacements greater than the error of 100 nm in at least two image frames and are color coded in red as "moving" nanocars. (C) Single molecule trajectory of the nanocar indicated by the red circle in panel A. Displacements as large as 500 nm between frames far exceed the changes in position recorded for the representative TRITC molecule labeled with the green circle in panel B (upper left-hand corner in panel C; note the scale bar). (D) Squared displacements SD (r^2) calculated from the single nanocar trajectory in (C) vs time. A linear fit according to SD = $4dt$ yields a squared displacement rate d of 6.7×10^{-16} m^2/s. The inset shows a scatter plot of the linear displacements between images for each of the five "nonmoving" molecules in (A). The 11 nm shift between the blue and red points, corresponding to the origin and the mean position, confirms a negligible sample drift.

tional dynamics on the 1−100 ms time scale and is much slower than a bond rotation. In contrast, only TRITC did not rotate as the polarization anisotropy values for TRITC (Figure 3B) ranged from −1 to 1 consistent with a random and stationary distribution of molecular orientations.[20,21] The fact that the molecules rotate is not surprising, considering that previous STM results[15] showed a combined pivot and translation motion of fullerene-wheeled nanocars on the nanometer length scale due to an independent wheel movement. The roughness of the glass surface is likely to further enhance pivoting of the nanocars.

Given the lack of long-range directionality, we analyzed the single nanocar trajectories to obtain displacement rates in analogy to two-dimensional surface diffusion.[22] Figure 2D shows the squared displacement SD of a single nanocar *versus* time as obtained from the trajectory in Figure 2C. A linear fit according to SD = $4dt$ yields a squared displacement rate d of 6.7×10^{-16} m^2/s. A histogram of single molecule diffusion constants is shown in the inset of Figure 3C. The average single molecule squared displacement rate of 2.2×10^{-16} m^2/s agrees well with the diffusion constant D of 2.7×10^{-16} m^2/s calculated from a mean squared dis-
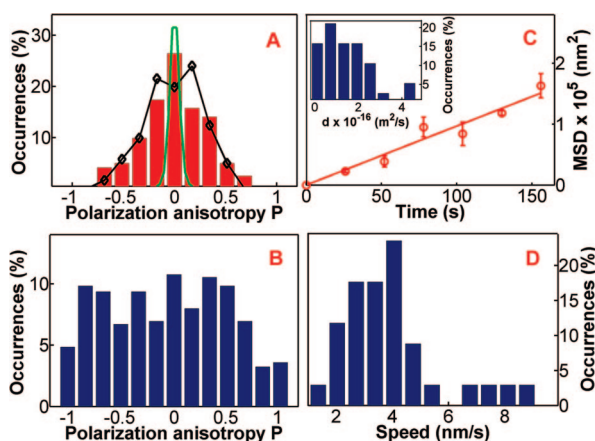
Figure 3. (A) Polarization anisotropy distribution of moving four-wheeled nanocars (red bars). The polarization anisotropy values are peaked at zero, indicating rotation of the nanocars during the image acquisition time. Rotation much faster than the acquisition time would result in the distribution given by the green line for shotnoise limited polarization detection. The black points and line are a simulation of the polarization anisotropy distribution for random hopping with a minimum rate of 10 hops per second, assuming an equal weight for all hopping directions. Please note that the polarization distribution is also consistent with a rolling and continuous pivoting motion. (B) Polarization anisotropy distribution of TRITC confirming the absence of rotational motion during the image acquisition time. (C) Mean squared displacement MSD ($\langle r^2 \rangle - \langle r \rangle^2$) *versus* time for all moving nanocars. A linear fit according to MSD = 4Dt yields a two-dimensional diffusion constant D of $2.7 \times 10^{-16} \pm 0.4$ m²/s. The inset shows a histogram of single molecule squared displacements rates d calculated from individual trajectories such as the one shown in Figure 2D. (D) Distribution of speeds of individual moving nanocars. The average speed of the nanocars is 4.1 nm/s or two nanocar lengths per second.

placement (MSD) analysis (MSD = 4Dt, Figure 3C). We also calculated the average minimum speed of the four-wheeled nanocars at room temperature and found a value of 4.1 nm/s (Figure 3D). On the basis of a diameter of 0.8 nm for a carborane wheel and assuming here that the translation was purely due to a rolling mechanism, a minimum wheel rotation frequency of 2 rotations per second was calculated. In contrast, fullerene-wheeled nanocars on a gold surface only moved after increasing the temperature to 500 K.[15] The difference is due to the much larger surface interaction energy of 200−250 kJ/mol per fullerene wheel on gold.[23,24]

Instead of a wheel-like rolling motion, the nanocars could also translate by hopping as has been observed for a large organic molecule such as hexa-*tert*-butyldecacyclene (HtBDC, $C_{60}H_{66}$), on Cu (110) by STM imaging.[25] We evaluated this scenario using the measured diffusion constant and estimating a minimum hopping rate based on the polarization anisotropy distribution of the nanocars. A simulation of the polarization anisotropy distribution (Figure 3A), assuming random hopping with an equal weight for all directions, gives a minimum hopping rate h of 10 hops per second. According to $D = 1/4\ \lambda^2 h$,[26] a maximum hop length λ of 10 nm is calculated, which is several times the size of the nanocar. If the nanocars are unable to ro-

tate freely while hopping, the hopping rate increases and the step size decreases, which eventually will become indistinguishable from a sliding or rolling motion.

Using a simple model, we can estimate the contributions due to rolling and hopping of the nanocars based on the activation energy for translational motion, which can be estimated from the measured diffusion constant D according to $D = D_0 \exp(-E/kT)$.[26,27] Here, T is the temperature and k the Boltzmann constant. D_0 is the two-dimensional diffusion constant of the nanocar in air given by the Stokes−Einstein diffusion equation $D_0 = kT/4\pi\eta a$ where η is the viscosity of air and a is the radius of the nanocar. If the motion of the nanocar molecule on the surface were free it would have a diffusion constant D_0. However, because of interactions with the surface the diffusion is significantly smaller. This model yields an activation energy E of 42 ± 5 kJ/mol at room temperature. For a carborane wheel to sit on a surface, three hydrogen atoms are necessary to bond to the substrate, which is illustrated in Figure 4A together with a suggested rolling mechanism. The bond strength between a carborane hydrogen and an oxygen atom on the glass surface is estimated to be 4.8 kJ/mol.[28] For the nanocar to roll it has to break one hydrogen bond per wheel and overcome a rotational energy barrier of 4.2 kJ/mol per bond connecting the wheel to the chassis,[29] which equals a total energy of 36 kJ/mol for a total of four wheels per car, in good agreement with the measured activation energy. On the other hand, if the nanocars were hopping, 12 hydrogen bonds have to be broken yielding an activation energy of 57 kJ/mol. This exceeds the experimentally measured value making hopping the less likely mechanism.

To further test this assignment, we measured single molecule trajectories and polarization anisotropy distributions for a TRITC-labeled three-wheeled nanocar, (Figure 4B). Compared to the four-wheeled car, the trimer nanocar is expected to have only 75% of the interaction energy with the glass surface and would therefore be more likely to hop assuming that the interaction of the dye label with the surface is comparable. However, we found no movement of the trimer nanocars as the trajectories were similar to those measured for TRITC only or the nonmoving four-wheeled nanocars. In addition to the absence of any translational movement in the trimer nanocars, we also did not observe rotational motion as confirmed by the polarization anisotropy distribution obtained from the fluorescence images (Figure S3) and the absence of a change of polarization anisotropy between image frames (Figure 4C). Although the trimer nanocar is expected to rotate, an important difference between the two nanocars is that TRITC is attached directly to the wheel of the trimer nanocar (Figures 1A and 4B) and could hinder a free wheel rotation. To test this hypothesis and to examine a possible role of the dye label on the nanocar move-
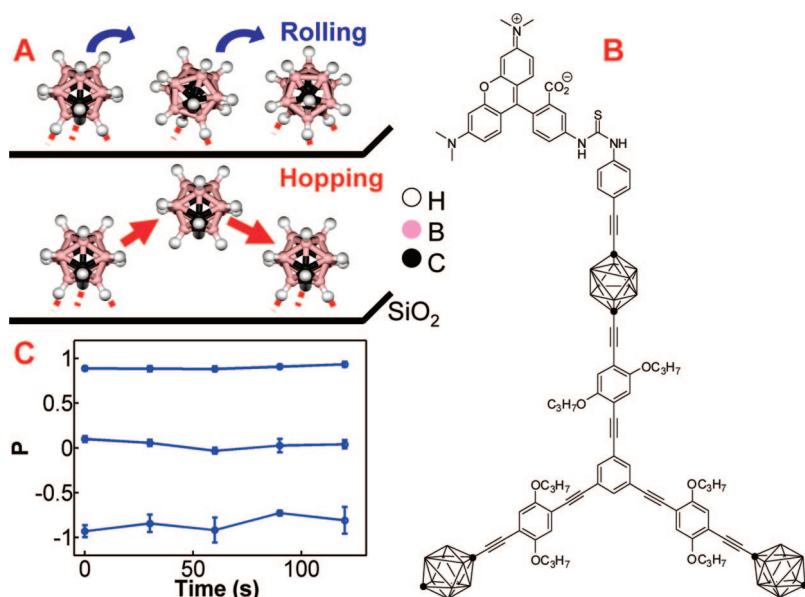
Figure 4. (A) Schematic comparison of a carborane wheel rolling (top) vs hopping (bottom). A wheel on the glass surface forms three hydrogen bonds with the oxygen atoms (not shown for clarity) of the SiO$_2$. For rolling only one of the three hydrogen bonds has to break while for hopping the whole wheel has to detach from the surface. (B) Dye labeled three-wheeled nanocar. (C) Three representative polarization anisotropy time trajectories for trimer nanocars showing that rotational motion is absent on a time scale of several minutes. Similar results were also obtained for polarization measurements of nonmoving four-wheeled nanocars and TRITC only.

ment, we plan to also study nonlabeled nanocars in the future.

CONCLUSION

Using single molecule fluorescence imaging, we have observed micrometer movement of dye-labeled carborane nanocars on a glass surface at room temperature. Polarization-sensitive measurements showed that translation is coupled with rotational motion. By comparing the four-wheeled nanocars to a three-

wheeled nanocar analogue and the unbound dye molecules, we conclude that the translation of the nanocars is consistent with a wheel-like rolling mechanism. While atomic resolution as with STM is not possible using single molecule fluorescence imaging, the results presented here demonstrate that our approach yields complementary data and gives useful insights into the micrometer-scale motion of molecular machines.

It is interesting to speculate how a truly unidirectional motion of nanocars can be achieved. Our results suggest that the speed of the nanocars is dictated by the strength of the interactions between the nanocar wheels and the surface. Changing the surface should therefore have a large impact on the mobility of the

nanocars. However, even more important for a controlled directional motion seems to be the reduction of pivoting, which was found to occur with a minimum frequency of 10 turns per second for the carborane-wheeled nanocars on glass. An extended nanocar chassis with an increased even number of wheels should be less susceptible to random pivot motion caused by an independent wheel movement, but at the expense of a reduced speed due to a stronger surface attraction and increased entropy for synchronized bond rotations.

METHODS

Single molecule fluorescence imaging was performed on a home-built sample scanning confocal microscope consisting of a frequency doubled diode-pumped laser (Coherent, Verdi), an inverted microscope (Zeiss, Axiovert 200), and avalanche photodiode (APD) detectors. Samples were excited by circularly polarized 532 nm laser light with an average power of 500 nW focused to a diffraction limited spot size of 250−300 nm. To visualize the nanocars, a dye label (tetramethylrhodamine isothiocyanate, TRITC) was attached to the end of the nanocar chassis (Figure 1A). TRITC tagging of the nanocars was accomplished through an aniline-bearing nanocar reacting with the isothiocyanate residue on the fluorophore (see Supporting Information for synthesis and characterization). We confirmed that the photophysical properties of TRITC labeled nanocars are similar to those of TRITC. TRITC and TRITC-labeled nanocars were spincasted (3500 rpm for 90 s) on plasma cleaned coverslips (Fisher Scientific, 12-545-F) from DMF solution with concentrations of $10^{-10}-10^{-12}$ mol/L. Prior to spin-casting and plasma cleaning, the coverslips were sonicated in acetone for 15 min. Samples were mounted on a *xyz* piezo scanning stage (Physik Instrumente, P-517.3CL) connected to a surface probe microscope controller (RHK Technology, SPM 1000). Emitted fluorescence from individual molecules was collected by a 100× oil-

immersion objective with a numerical aperture of 1.3 (Zeiss, Fluar) and filtered by a dichroic mirror and a notch filter to reduce scattered laser light. Fluorescence images were constructed by scanning the sample across the excitation laser. Typical images had dimensions of 10 × 10 μm and consisted of 128 × 128 pixels with an integration time of 1 ms/pixel (Figure 1B). Matlab software was written to automatically identify the position of each molecule in every image frame. For polarization sensitive detection, the fluorescence was separated into orthogonally polarized components I_x and I_y using a polarizing beamsplitter and detected by two APDs. After integrating the intensities over an area of 5 × 5 pixels corresponding to size of a single molecule, the polarization anisotropy was calculated according to $P = (I_y - I_x)/(I_y + I_x)$. For all of the samples studied we have measured about 200 molecules in order to extract statistically meaningful values.

Technology for technical support with minimizing the acquisition time for a single image frame.

Supporting Information Available: Synthesis and characterization of dye-labeled nanocars including ^{1}H NMR spectra and single molecule analysis of the nanocar directionality (Figure S1), polarization distribution of the "moving" nanocars (Figure S2), and polarization distribution of trimer nanocars (Figure S3). This material is available free of charge *via* the Internet at http://pubs.acs.org.

REFERENCES AND NOTES

1. van Delden, R. A.; ter Wiel, M. K. J.; Pollard, M. M.; Vicario, J.; Koumura, N.; Feringa, B. L. Unidirectional Molecular Motor on a Gold Surface. *Nature* **2005**, *437*, 1337–1340.
2. Fletcher, S. P.; Dumur, F.; Pollard, M. M.; Feringa, B. L. A Reversible, Unidirectional Molecular Rotary Motor Driven by Chemical Energy. *Science* **2005**, *310*, 80–82.
3. Leigh, D. A.; Wong, J. K. Y.; Dehez, F.; Zerbetto, F. Unidirectional Rotation in a Mechanically Interlocked Molecular Rotor. *Nature* **2003**, *424*, 174–179.
4. Kelly, T. R.; De Silva, H.; Silva, R. A. Unidirectional Rotary Motion in a Molecular System. *Nature* **1999**, *401*, 150–152.
5. Badjic, J. D.; Balzani, V.; Credi, A.; Silvi, S.; Stoddart, J. F. A Molecular Elevator. *Science* **2004**, *303*, 1845–1849.
6. Bissel, R. A.; Cordova, E.; Kaifer, A. E.; Stoddart, J. F. A Chemically and Electrochemically Switchable Molecular Shuttle. *Nature* **1994**, *369*, 133–137.
7. Brouwer, A. M.; Frochot, C.; Gatti, F. G.; Leigh, D. A.; Mottier, L.; Paolucci, F.; Roffia, S.; Wurpel, G. W. H. Reversible Translational Motion in a Hydrogen-Bonded Molecular Shuttle. *Science* **2001**, *291*, 2124–2128.
8. Perez, E. M.; Dryden, D. T. F.; Leigh, D. A.; Teobaldi, G.; Zerbetto, F. A Generic Basis for Some Simple Light-Operated Mechanical Molecular Machines. *J. Am. Chem. Soc.* **2004**, *126*, 12210–12211.
9. Serreli, V.; Lee, C.-F.; Kay, E. R.; Leigh, D. A. A Molecular Information Ratchet. *Nature* **2007**, *445*, 523–527.
10. Bedard, T. C.; Moore, J. S. Design and Synthesis of Molecular Turnstiles. *J. Am. Chem. Soc.* **1995**, *117*, 10662–10671.
11. Muraoka, T.; Kinbara, K.; Aida, T. Mechanical Twisting of a Guest by a Photoresponsive Host. *Nature* **2006**, *440*, 512–515.
12. Liu, Y.; Flood, A. H.; Bonvallet, P. A.; Vignon, S. A.; Northrop, B. H.; Tseng, H.-R.; Jeppesen, J. O.; Huang, T. J.; Brough, B.; Baller, M.; *et al.* Linear Artificial Molecular Muscles. *J. Am. Chem. Soc.* **2005**, *127*, 9745–9759.
13. Morin, J.-F.; Sasaki, T.; Shirai, Y.; Guerrero, J. M.; Tour, J. M. Synthetic Routes toward Carborane-Wheeled Nanocars. *J. Org. Chem.* **2007**, *72*, 9481–9490.
14. Shirai, Y.; Morin, J.-F.; Sasaki, T.; Guerrero, J. M.; Tour, J. M. Recent Progress on Nanovehicles. *Chem. Soc. Rev.* **2006**, *35*, 1043–1055.
15. Shirai, Y.; Osgood, A. J.; Zhao, Y.; Kelly, K. F.; Tour, J. M. Directional Control in Thermally Driven Single-Molecule Nanocars. *Nano Lett.* **2005**, *5*, 2330–2334.
16. Gimzewski, J. K.; Joachim, C. Nanoscale Science of Single Molecules Using Local Probes. *Science* **1999**, *283*, 1683–1688.
17. Yildiz, A.; Tomishige, M.; Vale, R. D.; Selvin, P. R. Kinesin Walks Hand-over-Hand. *Science* **2004**, *303*, 676–679.
18. Thompson, R. E.; Larson, D. R.; Webb, W. W. Precise Nanometer Localization Analysis for Individual Fluorescent Probes. *Biophys. J.* **2002**, *82*, 2775–2783.
19. Qu, X.; Wu, D.; Mets, L.; Scherer, N. F. Nanometer-Localized Multiple Single-Molecule Fluorescence Microscopy. *Proc. Natl. Acad. Sci. U.S.A.* **2004**, *101*, 11298–11303.
20. Forkey, J. N.; Quinlan, M. E.; Goldman, Y. E. Protein Structural Dynamics by Single-Molecule Fluorescence Polarization. *Prog. Biophys. Mol. Biol.* **2000**, *74*, 1–35.
21. Ha, T.; Laurence, T. A.; Chemla, D. S.; Weiss, S. Polarization Spectroscopy of Single Fluorescent Molecules. *J. Phys. Chem. B* **1999**, *103*, 6839–6850.
22. Schmidt, T.; Shultz, G. J.; Baumgartner, W.; Gruber, H. J.; Schindler, H. Imaging of Single Molecule Diffusion. *Proc. Natl. Acad. Sci. U.S.A.* **1996**, *93*, 2926–2929.
23. Altman, E. I.; Colton, R. J. Nucleation, Growth, and Structure of Fullerene Films on Au(111). *Surf. Sci.* **1992**, *279*, 49–67.
24. Akimov, A. I.; Nemukhin, A. V.; Moskovsky, A. A.; Kolomeisky, A. B.; Tour, J. M. Molecular Dynamics of Surface-Moving Thermally Driven Nanocars. *J. Chem. Theor. Comp.* **2008**, *4*, 652–656.
25. Schunack, M.; Linderoth, T. R.; Rosei, F.; Laegsgaard, E.; Stensgaard, I.; Besenbacher, F. Long Jumps in the Surface Diffusion of Large Molecules. *Phys. Rev. Lett.* **2002**, *88*, 156102/1–156102/4.
26. Rosei, F.; Schunack, M.; Naitoh, Y.; Jiang, P.; Gourdon, A.; Laegsgaard, E.; Stensgaard, I.; Joachim, C.; Besenbacher, F. Properties of Large Organic Molecules on Metal Surfaces. *Prog. Surf. Sci.* **2003**, *71*, 95–146.
27. Atkins, P.; de Paula, J. *Physical Chemistry*, 7th ed.; Freeman and Company: New York, 2002; Chapter 28.
28. Andrews, P. C.; Hardie, M. J.; Raston, C. L. Supramolecular Assemblies of Globular Main Group Cage Species. *Coord. Chem. Rev.* **1999**, *189*, 169–198.
29. Shirai, Y.; Osgood, A. J.; Zhao, Y.; Yao, Y.; Saudan, L.; Yang, H.; Chiu, Y.-H.; Alemany, L. B.; Sasaki, T.; Morin, J.-F.; *et al.* Surface-Rolling Molecules. *J. Am. Chem. Soc.* **2006**, *128*, 4854–4864.